Fabrication of Carbon/Silica Hybrid Materials Using Cationic Polymerization and the Sol-Gel Process

Stefan Spange, Hardy Müller, Christian Jäger[#], and Cornelia Bellmann[§]*

Department of Polymer Chemistry, Institute of Chemistry, Chemnitz University of Technology, Straße der Nationen 62, 09111 Chemnitz, Germany
[#] Institute of Physics, Friedrich-Schiller-University Jena, Max-Wien-Platz 1, D-07743 Jena, Germany
[§] Institute of Polymer Research, Hohe Straße 6, Dresden, Germany

Summary: Silica particles with different morphology have been functionalized with carbon shells by different synthetic procedures. In the key step, the bare silica particles are functionalized by a specific cationic surface polymerization with furfuryl alcohol (FA). The polyfurfuryl alcohol (PFA)/silica hybrid particles have been also post-functionalized with maleic anhydride (MSA) by a Diels Alder reaction. Simultaneously occuring cationic polymerization of FA and sol-gel process with TEOS has been used for producing interpenetrating carbon-silica hybrid materials. The thermal transformation of the PFA component on silica into the carbon phase has been carried out under argon atmosphere in a temperature range from 700 °C to 900 °C. The influence of the former morphology of the silica on the homogenity of the resulting carbon layer is shown by zetapotential measurements and electron microscopic investigations.

Introduction

Carbon and silica play an important role in chemistry, physics, and materials science due to their relevance in practical applications and academic research. More than a thousand original papers, books, and reviews on this topic have been reported (see [1-3] and [4-5] and the references therein).

Carbon exhibits a very rich structural and surface chemistry. [1-3, 6-10] Various different architectures are possible because carbon can be bound in linear (sp), trigonal (sp^2), and tetrahedral (sp^3) coordination.[2] Many crystalline and amorphous forms have been synthesized such as films, fibres, glassy carbon or nanotubes. [1-3, 6-8] Graphite like materials are widely interesting because of their high electrical conductivity, intercalating capability, high thermal stability, and high resistance towards organic solvents. [6-8]

 CCC 1022-1360/00/$ 17.50+.50/0

Hybrid materials consisting of a graphite like carbon phase and an inorganic oxidic component can be synthesized by different strategies. A convenient route for synthesizing the carbon component is the thermal transformation of a suitable organic precursor polymer into the carbon phase. [6-8, 11-21] Interpenetrating carbon/silica hybrid materials have been obtained by a sol-gel process of tetraalkoxysilanes using water soluble monomers or oligomers which are suitable as carbon precursor materials. [18-21] These materials are important for various applications, because each component serves as the template for the other one. Removing of any component results in a porous carbon and silica material, respectively. [20, 21]
In this paper we report on two different methods for producing carbon/silica hybrid materials. Carbon coated silica particles have been synthesized by method **A** and interpenetrating carbon/silica hybrid materials by method **B**.

A: Specific cationic surface polymerization of furfuryl alcohol (FA) on silica particles has been used for producing polyfurfuryl alcohol (PFA) coated silica hybrid precursors,[22, 23] because PFA has been well established as suitable precursor polymer for producing different kinds of carbon materials (scheme 1).

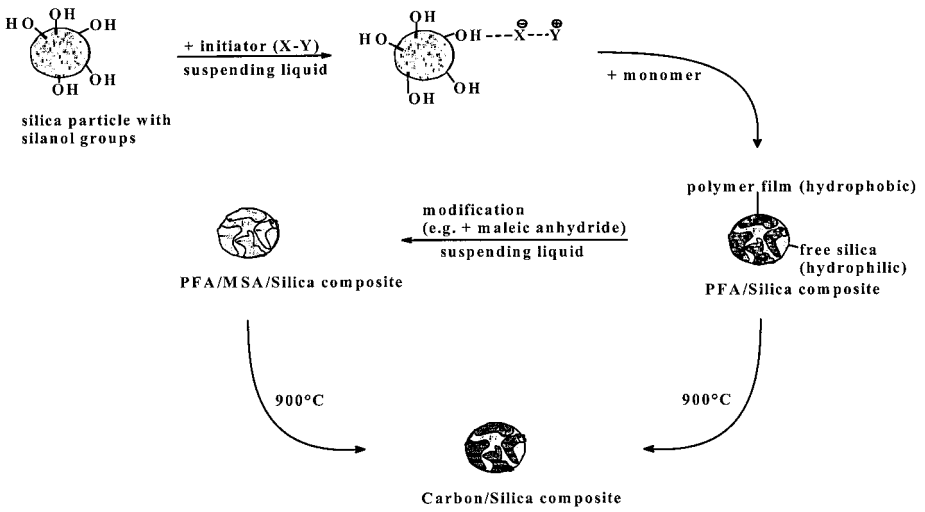

Scheme 1. Functionalization of silica particles by cationic surface polymerization.

B: Cationic oligomerization of FA is also possible in a tetraethoxysilane (TEOS)/water mixture. Due to the high stability of the furfurylium ion, it co-exists in sol-gel processes even in the presence of water which is suitable for synthesizing oligo FA simultaneously during the sol-gel process (scheme 2).

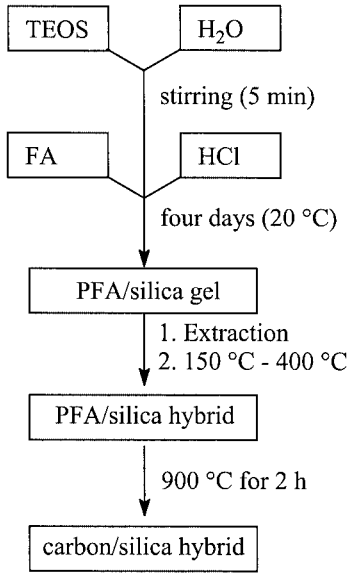

Scheme 2. Pathway for producing carbon/silica hybrid materials from FA and TEOS.

Experimental Section

The general procedure for the synthesis of PFA modified silica particles have been reported in the refs. [23, 24].

The postderivatization of the PFA/silica particles with MSA has been carried out in xylene as solvent. The structure analysis has been previously reported in a recent paper by Günther. [25]

The carbonization of the resultant PFA/silica and PFA-MSA/silica particles has been carried out as follows. The sample was heat-treated at a linear rate of 10 °C /min to 900 °C and held there for 3h to carbonize completely the polymer on the silica surface under inert atmosphere. The carbon contents were also analyzed by quantitative elemental analysis.

Solid state NMR spectroscopy, Raman spectroscopy, scanning electron microscopy, zetapotential and BET measurements have been performed as reported in the refs. [20, 23, 24, 26].

Results and Discussion

Cationic polymerization of FA in the presence of silica

For this work we used different kind of bare silica particles for functionalization, irregular particles with random size shape [KG 60, Merck®, particle diameter: 40 - 60 μm; specific surface (BET): 423 m^2/g; high porosity; pore volume: 0.71 - 0.78 ml/g] and spherical particles [Purospher® Si 80 **(PSP)** from Merck®, particle diameter: 5 μm; specific surface (BET): 405 m^2/g], of high purity and high quality in morphology (see experimental part). The cationic polymerization of FA on the surface of silica particles as well as in the sol-gel reaction mixture and the associated structure formation of PFA are strongly dependent on the experimental conditions for the polymerization.[24] The main important influence is that of reaction temperature. A higher temperature is responsible that formation of branched and conjugated sequences are improved, whereas ether bridges formation [-(C_4H_2O)-CH_2-O-CH_2-(C_4H_2O)]- is suppressed. For this report, we have selected the results from the optimized experiments. Therefore, we have used preferably those PFA/silica hybrid batches which have been synthesized at higher reaction temperature.

The solid state MAS CP {^{1}H} ^{13}C NMR analyses of the PFA/silica hybrid particles clearly demonstrates that PFA has been formed.[27] The PFA modified silica particles can be readily chemically post-functionalized by a Diels-Alder reaction with maleic anhydride (MSA) (see experimental part). The resulting materials are denoted as PFA-MSA/silica particles. The surface structure characterization of the PFA-MSA/silica material was also carried out with solid state ^{13}C NMR spectroscopy. Figure 1 shows the assignment of the ^{13}C NMR signals found in the solid state MAS CP {^{1}H} ^{13}C NMR spectrum of PFA-Silica hybrid- and of maleic acid functionalized PFA-Silica hybrid particles (MSA-PFA/silica).

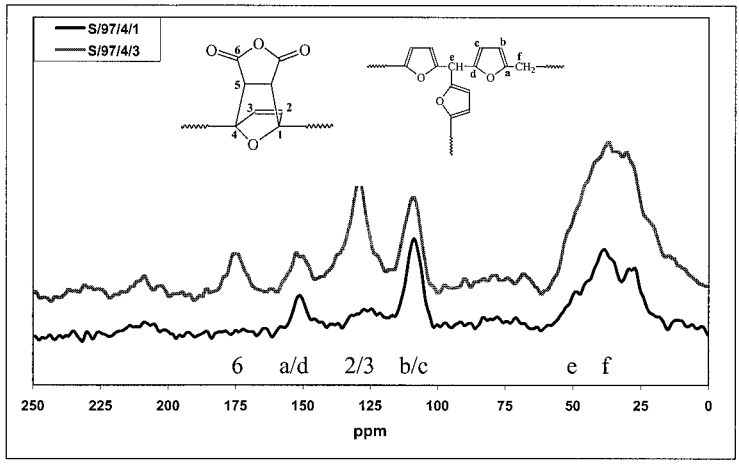

Figure 1. Molecular structures of the PFA network on the silica particle surface and assignment of the functional groups to the signals appearing in the solid state MAS CP ^{13}C {^{1}H} NMR spectra of the hybrid particles.

The -[-C_4H_2O-CH_2-]- chains can be evidenced in the solid state NMR spectra by the ^{13}C signals at about δ = 151 ppm, δ = 108-111 ppm, and δ = 28 ppm relating to the carbon atoms of the furan ring C2 / C5, C3 / C4, and the methylene bridge, respectively (see Figure1). The signal at δ = 39 ppm indicates crosslinking between oligoFA sequences. [27] The structure of the resulting PFA on silica is not uniform. However, the expected -(CH_2-C_4H_2O)- units are mainly present beside conjugated sequences which are formed by hydride transfer and isomerization reaction during the cationic surface polymerization. The conjugated sequences are responsible for the dark brown colour of the cationically synthesized PFA/silica hybrid particles. However, the concentration of the conjugated sequences are too low to be detectable by solid state NMR spectroscopy. When FA is simultaneously co-polymerized in the sol-gel process, then the fraction of conjugated sequences formed is evidently larger. This has been suggested by the solid state ^{13}C NMR spectrum of the interpenetrating PFA/silica network (Fig. 2).

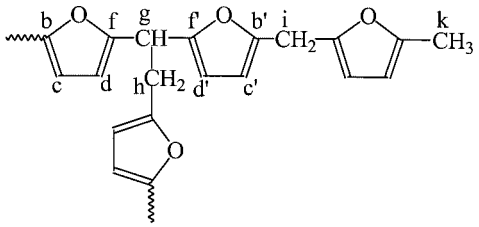

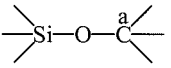

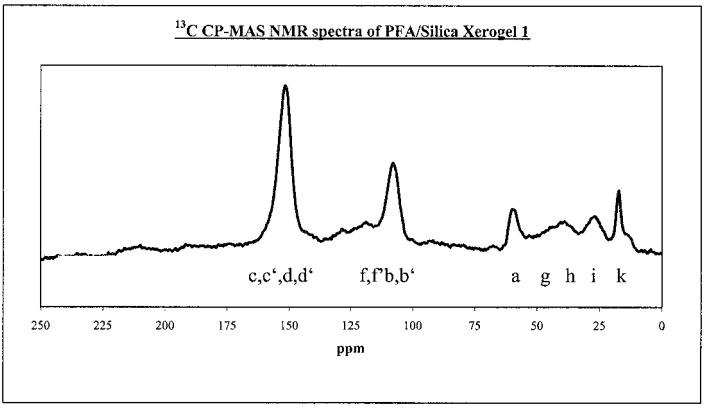

Figure 2. Solid state MAS CP {^{1}H} ^{13}C spectrum of an interpenetrating PFA/silica hybrid material as obtained by the HCl induced simultaneously occuring cationic polymerization of FA and sol-gel process with TEOS and water at 293 K. The carbon content of the hybrid is about 18 %.

Beside the expected -[-C_4H_2O-CH_2-]$_n$- chain sequences, which can also be evidenced in the solid state NMR spectra by the ^{13}C signals at about δ = 151 ppm, δ = 108-111 ppm, and δ = 28 ppm, (see Figure 2), a further rather intense signal at about δ = 60 ppm indicates Si-O-C bonds [28] and the broad signal at δ = 39 ppm indicates the crosslinking between oligoFA sequences. The main part of the PFA fraction cannot be removed from the xerogel by an extraction with organic solvents (methanol, 1,2-dichloroethane) or water. Furthermore, a ^{13}C signal hinting at methyl groups is found at δ = 17.5 ppm.

The solid state ^{1}H MAS NMR spectrum of the PFA/silica hybrid xerogel gave no detailed structure information. Broad signals for the protons of the furan ring at about δ = 5.95 ppm and δ = 1.1 ppm for methyl groups are observed as well as rather wide signals at δ = 3.95 ppm which cannot be assigned to specific structure elements because of silanol groups, water, and possible TEOS residuals. The methyl groups may be formed by a hydride transfer reaction

from the methylene bridges of oligoFA to cationically active oligofurfurylium intermediates. However, signals for Si-O-C bonds as well as methyl groups in the solid state NMR spectra can also be caused by TEOS residuals in the polyFA/silica xerogel. The high content of methyl head groups in the FAoligomers would be consistent with the black color of oligoFA, because the hydride transfer reaction is responsible for the formation of the conjugated sequences. The ^{13}C signals for the olefinic carbon atoms are not resoluted, but they are clearly detectable in the solid state ^{13}C $\{^1H\}$ NMR spectrum as a broad signal between $\delta = 120$ and $\delta = 140$ ppm. The cationically conjugated sequences are responsible for the dark green color of the PFA/hybrid gel [$\lambda = 600$ nm and a shoulder at about $\lambda = 765$ nm]. Because conjugated polymers are especially suitable precursor polymers for producing carbon, the PFA cationically produced on silica particles and among the sol-gel process, respectively, is advantaged for this purpose.

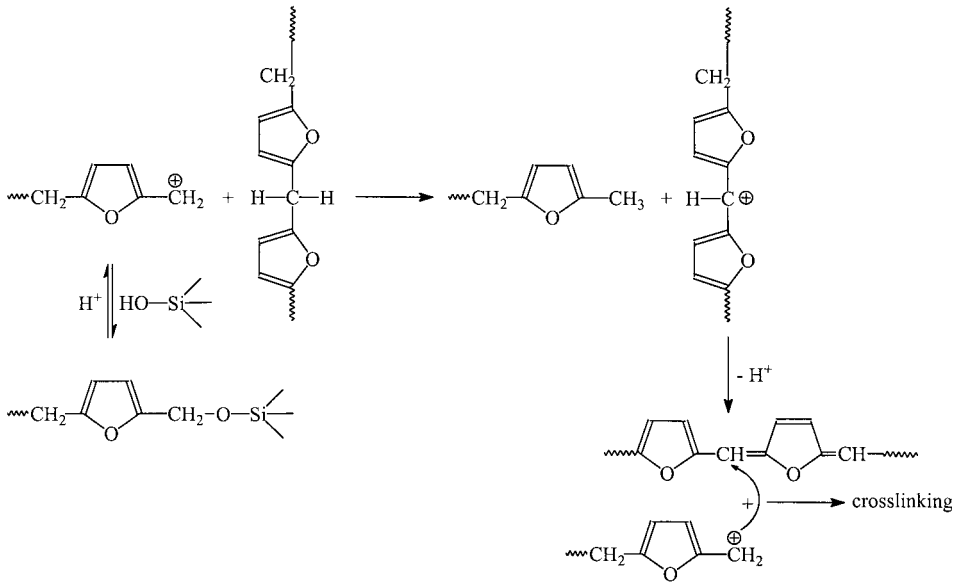

Chart 1. Theoretically possible reactions of the cationically active polyfurfurylium chain with PFA, conjugated sequences, and the silanol groups formed during the sol-gel process.

Both kind of precursor materials PFA/silica or PFA-MSA/silica and the PFA/silica xerogel have been used for the carbonization procedure in this paper.

900 °C has been found to be an optimized carbonization temperature for both kinds of precursor materials MSA-PFA/silica or PFA/silica and PFA/silica xerogels. Using this

optimized temperature, the carbonization reaction proceeds to is completion, because the IR signals derived from the precursor polymers are disappeared completely in the DRIFT-spectrum. A higher carbonization temperature than 900 °C is not suitable, because then the BET-surface area of the porous carbon/silica particles decreases significantly due to changes of the morphology of the silica frame. [24]

Carbon/silica particles

When above 12 % weight of carbon are present on the carbon/silica hybrid particles surface, the silanol groups completely disappear as seen by the lack of the single valency vibration of the silanol groups at $\nu = 3740\ cm^{-1}$ in the DRIFT spectrum.
We presume that the MSA functionalized PFA/silica particles are better suited for the carbonization reaction since the thermal cleavage of the anhydride groups should occur even at lower carbonization temperature resulting in CO_2 and aromatic rings. The surface carbonization process transforming PFA into carbon also proceeds very effectively since conjugated sequences are present in the precursor polymer. We think that the former conjugated sequences in the PFA layer on silica serve like a seed for producing carbon germs during the first stage of carbonization.

These germs are present in high concentrations which significantly improve the carbonization reaction. We think that these both facts are responsible for the high yield of the carbon phase. The formation of the carbon phase among the silicatic frame is clearly shown by Raman spectroscopy. [20, 30,31] The results of Raman as well as EPR spectroscopic investigations (the evident signal at g = 2.00027 [G] indicates paramagnetism) show the graphite like property of the carbon layer. The carbon/silica particles produced from MSA-PFA/silica show the highest conductivity which supports that a graphite like carbon layer has been formed. The difference of conductivity compared to carbon/silica from PFA/silica is significant. Qualitative indicative results are shown in Figure 3.

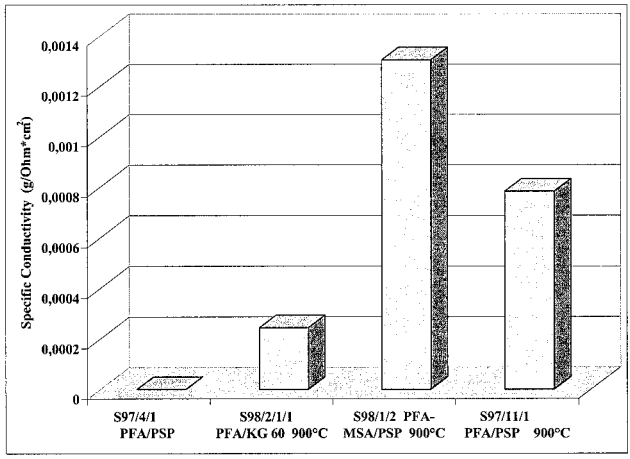

Figure 3. Conductivity of PFA functionalized silica particles (S97/4/1) Carbon coated Purospher® particles using PFA/silica(KG 60) (S98/2/1/1), Carbon coated Purospher® particles using PFA/PSP precursor (S97/11/1) and MSA-PFA/PSP precursor (S98/1/2). (PSP = porous silica particle).

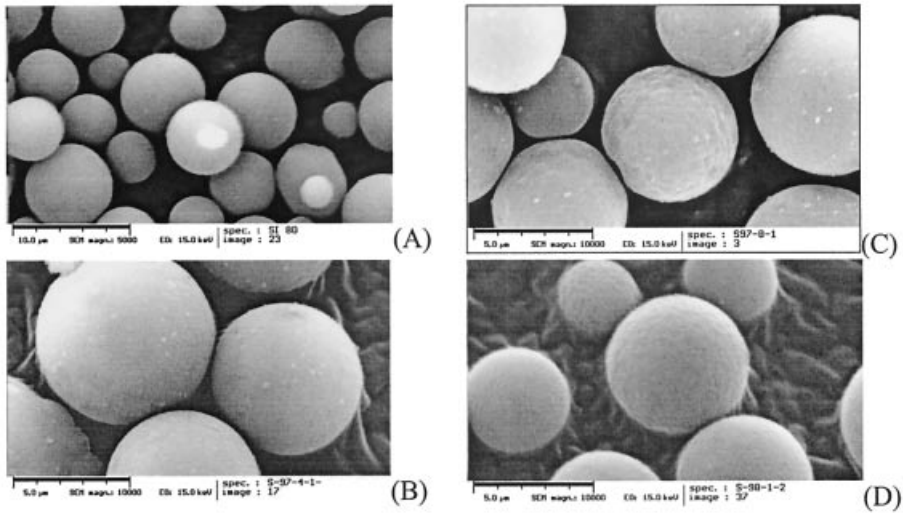

Figure 4. Scanning electron microscopic (SEM) pictures of
(A) bare Purospher® silica particles
(B) PFA functionalized silica particles
(C) carbon coated Purospher® particles using PFA/silica as precursor
(D) carbon coated Purospher® particles using MSA-PFA/silica as precursor.

The scanning electron microscopic (SEM) pictures taken from the functionalized silica particles studies show that the shape and the morphology of the former silica frame is not changed by the surface modification reactions (Fig. 4). This result has been found independent of the kind of silica particle used for the derivatization reaction. Especially, the carbon layer derived from the former MSA functionalized PFA/silica particles show a "tennis ball" like morphology. Compared to the former silica particles surface, the size and shape of the particle remain unchanged. The IR results show, that neither free silica batches nor holes in the carbon shell are present. Of course, sometimes (very rarely) a broken hybrid particle is observed among the nonbroken ones. But we think this is more likely due to mechanically induced influences rather than caused by the modification procedure

For detecting sensitive differences to the surface properties, zetapotential measurements have been well established for characterization of bare silica and functionalized silica particles as well as carbon. [26, 29] Figure 5a shows the zetapotential plots as function of pH for differently functionalized KG 60 silica samples and Figure 5b for the Purospher® silica particles (PSP) studied in this work.

Overall, for bare silica, the IEP is observed at pH = 2.8. Functionalization of silica with PFA causes no significant shift upon the IEP. This behavior is expected and shows that the surface charges in water are mainly determined by the residual silanol groups on the PFA/silica hybrid particles surface.[29] The post-functionalization of the PFA/silica hybrid particles with MSA causes a significant shift of the IEP to lower pH, at approximately pH = 2. This effect is well in accordance with the higher acidity of maleic acid in water (pK_s = 1.92 at 298 K) compared to that of silica (pK_s = 2.65).[29]

Generally, for the carbon/silica hybrid particles a significant shift of the IEP to higher pH is observed. The shift observed is different for the two silica samples used. It takes place from pH = 2 (MSA-PFA/silica) and pH = 2.8 (PFA/silica), respectively, to pH = 4 for carbon/silica KG 60. For comparison, (non derivatized) carbon fibres show the IEP at pH = 4.5 and qualitatively similar zetapotential plots as function of pH like the carbon/silica particles. [26] This comparison shows that the macroscopic surface properties of the carbon/silica KG 60 particles are mainly determined by the carbon layer and not by the silicatic core. The small difference of the IEP measured for pure carbon (IEP at pH = 4.5)[26] compared to carbon/silica (IEP at pH = 4) is caused by accessible weakly acidic groups which are likely operative at

edges and irregular sizes of the particles surface. They are not detectable by DRIFT spectroscopy.

The carbon/silica hybrid particles synthesized from PSP/silica show the IEP at pH = 4.5, which agrees with the expected value for the pure carbon phase. This result shows that a homogeneous carbon layer has been formed. Thus, the method described here is very suitable for producing carbon/silica particles with adjustable surface properties.

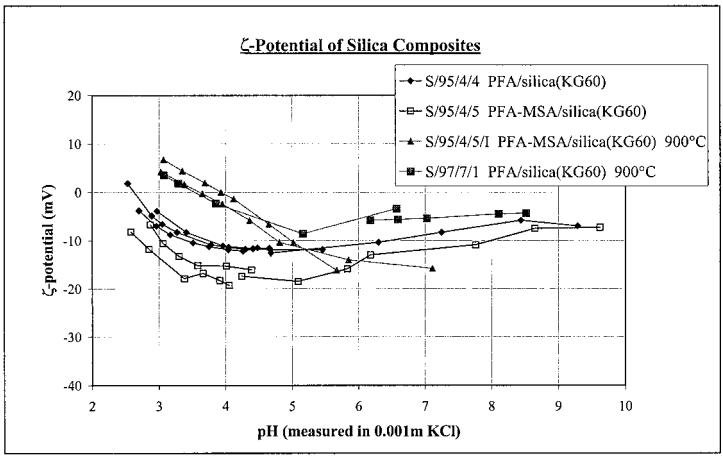

Figure 5a. Zetapotential plots of PFA/silica(KG 60) (-◆-), PFA-MSA/silica(KG 60) (-□-) and carbon/silica(KG 60) from PFA-MSA/silica precursor (-▲-) and from PFA/silica precursor (-■-) as function of the pH of the aqueous solution.

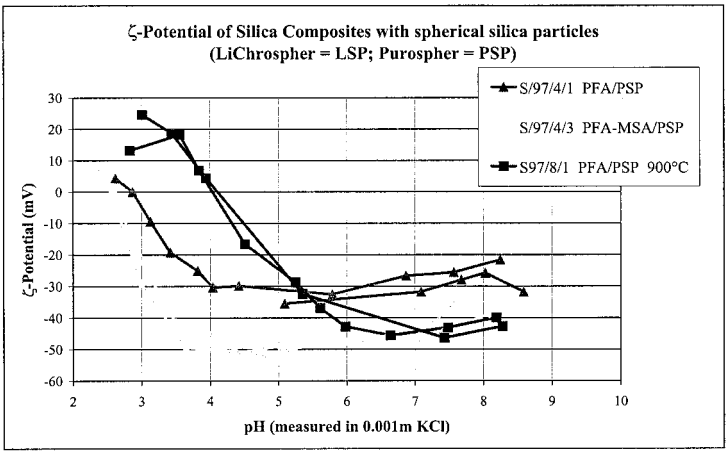

Figure 5b. Zetapotential plots of PFA/silica(PSP) (-▲-) PFA-MSA/ silica(PSP) (-◆-) and carbon/silica(PSP) from PFA/silica precursor (-■-) as function of the pH of the aqueous solution.

Interpenetrating carbon/silica monoliths

PFA/silica xerogel hybrid materials with different compositions can be synthesized by simultaneously occurring cationic polycondensation of FA and sol-gel process with TEOS.[20, 21] Those xerogel hybrid materials are suitable precursors for producing nanostructural carbon/silica materials by their thermal induced transformation at 900 °C under inert atmosphere. The structures of the two components among both the polyFA/silica xerogel and carbon/silica hybrid material have been confirmed by different spectroscopic methods. The formation of the carbon phase among the silicatic frame is clearly shown by Raman spectroscopy. [30, 31] The two characteristic bands for the carbon phase at $\nu = 1300$ cm^{-1} and $\nu = 1550$ cm^{-1} are clearly observed. Both Raman bands have the same intensity. This result of the Raman spectra suggest that the carbon phase is graphite like and non-porous. This is confirmed by attempts of BET measurements. A measurable BET surface area could not be determined for the carbon/silica hybrid material. It is lower than 1 m^2/g. The carbon phase can be burned with oxygen. Afterwards a porous silica is obtained which has a BET surface area of about 120 m^2/g. The silica phase shows a porous structure with mesopores in the range of 20 nm to 30 nm. The remaining silica phase obtained after the burning process contains nanopores with 2-3 nm size which amounts to about 80 % of the total pore volume. Inside the pores the polymer, respectively, the carbon phase is located (white colored sections in Figure 6). As a consequence, an interpenetrating network structure is formed (see Fig. 6).

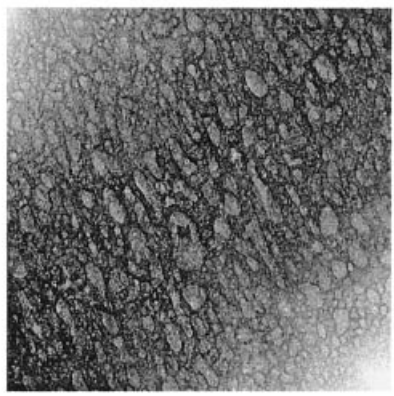

Figure 6. Electron micrograph of an interpenetrating carbon/silica hybrid material.

Thus, during the sol-gel process the two components formed PFA and silica, respectively, serve as a template for each other, which offers the opportunity in constructing new

mesoporous hybrid materials by removing the nondesired component either by HF (silica) or oxygen (carbon).

Acknowledgement

Financial support by the Fonds der Chemischen Industrie, Frankfurt/Main, and the University of Technology, Chemnitz, is gratefully acknowledged.
The authors thank Simone Kehr, Polymer Chemistry, for technical assistance and Prof. Dr. R. Holze, Electrochemistry, Technical University Chemnitz, for providing the equipment to do the conductivity measurements. We thank Dr. Manfred Friedrich, Insitute of Inorganic Chemistry, Friedrich-Schiller-University Jena, for recording and utilizing the EPR spectra.

References

(1) J.C., Bokros, In *Chemistry Physics of Carbon*; Walker, P., L., Jr., Ed..; Marcel Dekker: New York **1969**; *Vol.5*, 1-118.

(2) F. Diederich, Y. Rubin, *Angew. Chem.* **1992**, *104*, 1123-1292; Int. Ed. Engl. **1992**, *31*, 1101 and references cited therein.)

(3) T. W. Ebbesen, *Acc. Chem. Res.* **1998**, *31*, 558-566.

(4) R. P. W. Scott, *Silica Gel and Bonded Phases* , **1993**, John Wiley & Sons.

(5) R. K. Iler, *The Chemistry of silica*, 1979 John Wiley & Sons,New York.

(6) C.-C. Han, J.-T. Lee, R.-W. Yang, H. Chang, H., C.-H. Han, Chem. Commun. **1998**, 2087

(7) E. D. Miller, D. C. Nesting, J. V. Badding, Chem. Mater.**1997**, *9*, 18-22.

(8) O. Vohler, P.-L. Reiser, R. Martina, D. Overhoff, Angew. Chem. **1970**, *82*, 401-452.

(9) E. Fitzer, *Angew. Chem.* **1980**, *92*, 375-386.

(10) H. O. Böder, *Angew. Makromol. Chem.* **1982**, *109/110*, 125-138.

(11) J. Rodriguez-Mirasol, T. Cordero, L. R. Radovic, J. J. Rodriguez, *Chem. Mater.* **1998**, *10*, 550.

(12) T. Kyotani, T. Nagai, S. Inoue, A. Tomita, *Chem. Mater.* **1997**, *9*, 609.

(13) M. Narisawa, K. Yamane, Y. Okabe, K. Okamura, *J. Mater. Res.* **1999**, *14*, 4587.

(14) S. Han, T. Hyeon, *Chem. Commun.* **1999**, 1955.

(15) N. Sonoba, T. Kyotani, A. Tomita, *Carbon* **1988**, *26*, 573.

(16) T. Kyotani, N. Sonoba, A. Tomita, *Carbon* **1991**, *29*, 61.

(17) T. Kyotani, T. Nagai, S. Inoue, A. Tomita, A., *Chem. Mater.* **1997**, *9*, 609.

(18) S. M. Manocha, D. Y. Vashistha, L. M. Manocha, *J. Mater. Sci. Lett.* **1997**, *16*, 705.

(19) M. Narisawa, K. Yamane, Y. Okabe, K. Okamura, *J. Mater. Res.* **1999**, *14*, 4587.

(20) H. Müller, C. Jäger, P. Rehak, N. Meyer, J. Hartmann, S. Spange, *Adv. Mat.* **2000**, *12*, 1671.

(21) D. Kawashima, T. Aihara, Y. Kobayashi, T. Kyotani, A. Tomita, *Chem. Mat.* **2000**, *12*, 3397.

(22) A. Gandini, *Adv. Polym. Sci.* **1977**, *25*, 17.

(23) S. Spange, *Progr. Polym. Sci.* **2000** , *25*, 781-849.

(24) H. Müller, S. Spange, G. Marx, N. Meyer, I. Mehlhorn, C. Bellmann, Chem. Mat. 2001, submitted

(25) H. Günther, V. Franke, Fresenius *J. Anal. Chem.* **1997**, *357 (5),* 505.

(26) F. Simon, H. J. Jacobasch, D. Pleul, P. Uhlmann, *Progr. Coll. Polym. Sci.* **1996**, *101*, 184-188.

(27) S. Spange, H. Schütz, R. Martinez, *Makromol. Chem.* **1993**, *194*, 153.

(28) D. M. Hoebbel, D., M. Nacken, H. Schmidt, *J. Sol-Gel Sci. Techn.* **1998**, *12*, 169.

(29) F. Simon, H. J. Jacobasch, S. Spange, *Coll. Polym. Sci.* **1998**, *276*, 930-939.

(30) D. S. Knight, W. B. White, *J. Mater. Res.* **1989**, *4*, 385.

(31) T.-H. Ko, C.-Y. Chen, *J. Appl. Polym. Sci.* **1999**, *71*, 2219.